Received Date : 15-Mar-2016
Revised Date : 25-Aug-2016
Accepted Date : 23-Sep-2016
Article type : Research Article

The Photostabilizing Effect of Grape Seed Extract on Three Common Sunscreen Absorbers

Bice S. Martincigh * and Moses A. Ollengo

School of Chemistry and Physics, University of KwaZulu-Natal, Westville Campus, Private Bag X54001, Durban 4000, South Africa

*Corresponding author email: martinci@ukzn.ac.za (Bice S. Martincigh)

ABSTRACT

The photostabilizing ability of grape seed extract on three common sunscreen absorbers: 2-ethylhexyl-*p*-methoxcinnamate (EHMC), benzophenone-3 (BP3) and tert-butylmethoxy dibenzoylmethane (BMDBM), was investigated. Samples were exposed to simulated solar radiation and monitored by spectrophotometric and chromatographic methods. The chemical composition of the grape seed extract was determined by GC-MS and HPLC-MS and the major secondary metabolites were found to be epicatechin and catechin. Exposure of the extract to UV radiation increased the UV absorption capacity of the extract. All sunscreens showed an improved photostability in the extract. The inherent photo-instability of BMDBM when exposed to UV radiation was almost eliminated in the presence of grape seed extract. A

mixture of all three sunscreens in the extract showed very high photostability and a red shift covering the entire UVB and UVA regions thereby improving the broad-spectrum protection. The incorporation of grape seed extract in sunscreen and other cosmetic formulations for topical application boosts photoprotection by stabilizing the UV filters and enhancing broad-spectrum coverage. This in turn helps in reducing the amounts of absorbers and other additives incorporated in a sunscreen product and consequently lowers the risk of an unprecedented build-up of photoproducts whose toxicities are currently unknown.

INTRODUCTION

Human skin is the principal defence of the entire body against harmful environmental contaminants, various xenobiotic factors and exposure to solar ultraviolet (UV) radiation. The solar UV-spectrum can be divided into three regions: the UVC (< 280 nm), UVB (280-320 nm) and UVA (320-400 nm) bands (1, 2). Approximately 5% of the total solar UV radiation reaching the earth's surface falls in the UVB region. UVB radiation has been shown to possess suppressive effects on the immune system, as well as acting as a tumour initiator, tumour promoter and a co-carcinogen (3). Various biological effects including: inflammation, sunburn cell formation, hyperpigmentation, immunological changes, and induction of oxidative stress, have been associated with exposure to UVB radiation. These biological responses contribute to the development of the many forms of skin cancer (4, 5). Among the various forms of skin cancer, basal cell carcinoma (BCC) and squamous cell carcinoma (SCC), referred to as non-melanoma skin cancer, are by far the most common form of cancer in humans and account for approximately 80% and 16%, respectively, of reported cases (6). The remaining part of the solar UV radiation (about 90-95%) falls in the UVA region. UVA radiation has longer

wavelengths and correspondingly deeper penetration through the epidermis into the dermis. Exposure to UVA radiation induces the generation of singlet oxygen ($^1O_2$) and hydroxyl ($^{\cdot}OH$) free radicals, and a host of other reactive oxygen species (ROS), which can cause damage to cellular macromolecules, like proteins, lipids and DNA, and suppress some immunological functions (2, 3, 7-9). It is also thought to play some role in the initiation of the worst form of skin cancer, namely, malignant melanoma (5, 10, 11).

Thus, the adverse effect of UV radiation on human health and, particularly, the development of skin cancers cannot be overemphasized. There is therefore a need to develop efficient photoprotective and chemopreventive strategies to combat this hazard. The traditional approach has been the use of sunscreens incorporating both physical blockers and chemical absorbers in combination with other cosmetic agents. This approach has associated advantages and disadvantages; of prime concern is the photoinstability of some chemical absorbers (12) and the cutaneous permeation of physical blockers into the more labile tissues. In the case of chemical absorbers, the photoproducts of some of the commonly used sunscreen agents are unknown and correspondingly their effects are still a subject of further investigation. For the physical blockers commonly used, like titanium dioxide, their particle size is a major concern since the current use of nanoparticles poses the danger that these (< 100 nm) particles may permeate deep into the dermis and cause more harm by way of ROS generation. Consequently, various health regulatory authorities have set maximum allowed values of these agents in various cosmetic formulations. However, the standards vary greatly from region to region with the need for broad-spectrum protection and a high sun protection factor (SPF).

There is a growing trend of incorporating plant extracts in sunscreen formulations with the aim of reducing the amounts of the sunscreening agents. The plant extracts come with other ethnopharmacological benefits although most of them are not yet confirmed. One major advantage of plant extracts is that they have a long history of traditional use for treating various disorders with no adverse effects. However, caution needs to be exercised as some have also demonstrated fatal toxicities when administered at higher dose levels.

Among the extracts that have attracted scientific interest is the grape seed (*Vitis vinifera*) extract. A number of working groups have shown that grape seed extract products have beneficial effects on vascular disease and wound healing (13). There is a strong indication that these extracts play a preventive role against some cancers (14, 15). Results from both *in-vitro* and *in-vivo* models indicate that grape seed extract confers potent protection against oxidative stress and free radical-mediated tissue damage (3, 16). A major constituent of grape seed extract are proanthocyanidins. These are envisaged to inhibit enzymes intrinsic to the breakdown of the skin, such as collagenase, elastase, and hyaluronidase, and inhibit tumour growth (3). The proanthocyanidins present in grape seeds are known to have biological effects, including prevention of photocarcinogenesis (3, 17)

Proanthocyanidins occur naturally in a large variety of fruits, vegetables, nuts, seeds, flowers and bark. This class of phenolic compounds takes the form of oligomers or polymers of polyhydroxy flavan-3-ol units, such as (+)-catechin and (-)-epicatechin (18) (Fig. 1). The seeds of the grape are a particularly rich source of proanthocyanidins; the major component of polyphenols in red wine. These grape seed proanthocyanidins are mainly dimers, trimers and highly polymerized oligomers of monomeric catechins (19) (Fig. 1). Experimental work has shown proanthocyanidins from grape seeds to be potent antioxidants and free radical

scavengers, being more effective than either ascorbic acid or vitamin E (20-22). These secondary metabolites have been shown to have anti-carcinogenic activity in different cancer models (23, 24).

There is overwhelming interest in the use of botanicals for the prevention of various diseases; the main focus has been their consumption as dietary supplements. The topical application of plant extracts in combination with known sun active molecules in cosmetics (25) is on the rise but no literature is available on their actual role. The aim of this study was to investigate the effects of grape seed extract on the photostability of 2-ethylhexyl-*p*-methoxy cinnamate (EHMC), benzophenone-3 (BP3) and tert-butylmethoxy dibenzoylmethane (BMDBM).

MATERIALS AND METHODS

Materials. The grape seed extract was purchased from Warren Chem Specialities (Pty) Ltd, South Africa. The solvents, acetonitrile (ACN) and methanol (MeOH), of HPLC-grade were purchased from Merck KGaA. The three chemical UV filters of analytical purity (99.9%) were obtained as follows: 2-ethylhexyl-*p*-methoxcinnmate (EHMC) and tert-butylmethoxy dibenzoylmethane (BMDBM) were a kind donation from BASF, and benzophenone-3 (BP3) was purchased from Sigma-Aldrich. N,O-Bis(trimethylsilyl)trifluoroacetamide (BSTFA) was purchased from Supelco.

Characterisation of grape seed extract. The grape seed extract was characterised by gas chromatography-mass spectrometry (GC-MS), gas chromatography-flame ionisation detection (GC-FID), and high performance liquid chromatography-mass spectrometry (HPLC-MS) in order to identify the chemical components present.

Sample preparation. About 25 mg of grape seed extract powder was soaked in 25 mL of methanol at 25 °C and placed in an ultrasonic bath for two hours and then left to stand for 24 hours protected from light by aluminium foil. The extraction mixture was then made up to 50 mL in a volumetric flask with methanol. The resultant solution was filtered through a 0.45 µm Millipore Millex-LCR membrane filter and then transferred to an aluminium foil cased glass vial for storage. A 20 µL aliquot of this solution was injected into a HPLC-MS for characterisation of the chemical components in the extract. The remaining solution was preserved for photostability studies.

The grape seed extract samples for GC-MS characterisation were firstly derivatised to ensure volatilisation of the polyphenols in the extract. This was achieved by dissolving a sample mass of about 2 mg of extract powder in 1.0 mL of ACN in a clean, dry 3 mL reaction vial. To this solution, 0.5 mL of BSTFA was added, then capped tightly, mixed well, and heated at 70 °C for 45 min. The resultant derivatised mixture was filtered through a 0.45 µm Millipore Millex-LCR membrane syringe tip filter after cooling to room temperature. A volume of 0.1 µL of this derivatised sample was then injected into the GC-MS chromatograph.

GC-MS analysis. A 0.1 µL volume of the derivatised grape seed extract sample was delivered into a Shimadzu GC-MS (QP2010 SE), with a column temperature set at 70 °C and the injection port at 250 °C. Injections were in split mode at a ratio of 20:1. Components were separated in a GL Sciences InertCap 5MS/Sil 30 m × 0.25 µm quartz capillary column with a bound stationary phase consisting of 5% dimethylpolysilphenylenesiloxane. The column was held at 70 °C for 2 min, and then the temperature was increased to 240 °C at 10 °C min^{-1}, then held for 5 min, followed by an increase to 270 °C at 10 °C min^{-1} and held there for 10 min. The linear velocity was set at 30.0 cm

s^{-1}. The MS ion source temperature was 200 °C and the interface temperature was set at 250 °C. The MS detector was programmed to run in scan mode in the *m/z* range 35-1000 at a scan speed of 3333. The total run time was 37 min with helium as the carrier gas.

GC-FID analysis. To check method interconvertability a GC-FID experiment was carried out on the same samples (derivatised grape seed extract) with the same temperature program. The GC-FID used was a Shimadzu GC-2010, fitted with an AOC 20i autosampler and an AFC-2010 flow unit. Components were separated in a DB-5, 30 m × 0.25 µm quartz capillary column with a bound stationary phase consisting of 5% phenyl polysilphenylenesiloxane. The make-up gas was nitrogen/air flowing at 10 mL min^{-1}, the carrier gas was hydrogen with a flow rate of 40 mL min^{-1} and oxygen/air flowing at 400 mL min^{-1}. The injection port was set at 250 °C, operating in a split mode of 20:1 for an injection volume of 0.1 µL. The velocity flow control mode was adopted keeping the pressure at 61.9 kPa, the total flow rate at 5.0 mL min^{-1}, a column flow of 0.68 mL min^{-1}, and a linear velocity of 20.0 mL s^{-1}.

HPLC-MS analysis. The grape seed extract dissolved in methanol was characterised by means of HPLC-PDA-ESI-MS/MS. The analysis was carried out on an Agilent 1200 series LC MSD Trap, equipped with a photodiode array detector, a binary pump, a degasser, autosampler, and an ESI Trap MS. This employed a G1312A binary pump, a G1316A autosampler, a G1322A degasser and a G1315D photodiode array detector controlled by Chemstation software (Agilent, v.08.04). The chromatographic separation was achieved on an Agilent Zorbax Eclipse XDB C-18 reversed-phase column (150 × 4.6 mm, 5 µm particle size). The mobile phase was composed of water:formic acid (99:1, v/v solvent A) and acetonitrile (solvent B). The mixtures were resolved

by a gradient elution as follows: 5–13 min, 16% B; 13−18 min, 45% B and held for 5 min; 23−28 min, 75% B, held for 5 min; 33−40 min, 99% B, then held 5 min; and then dropped linearly to 16% B for 15 min. The experiment was performed at ambient temperature with a flow rate of 1 mL min^{-1} and an injection volume of 20 µL. The chromatograms were collected at detection wavelengths of 275, 280, 286, 310, 320 and 358 nm with a bandwidth of 4 nm simultaneously in each of the 60 min run time. The photodiode array detector was set to collect the UV-vis spectra of the chemical species separated over the range from 190 to 800 nm. Analyses were interfaced to an Agilent-SL LC MSD trap equipped with an electrospray ionization source and operated in the negative-ion mode. The mass detector was a G2445A ion-trap mass spectrometer controlled by LC-MSD software (Agilent, v.4.1). The nebulizing gas was nitrogen set at a pressure of 65 psi and a flow rate adjusted to 116 mL min^{-1}. A heated capillary and voltage was maintained at 350 °C and 4 kV respectively. The instrument was programmed to scan over a mass range from *m/z* 90 to 2000. The target ion accumulation in the trap was put at 30000 counts for a maximum accumulation time of 50 ms. MS^2 data were acquired in the negative ionization automatic smart mode to obtain MS^{n-1}; primary precursor ion. The target ion was set at *m/z* 350, the compound stability at 100%, and the trap drive level at 90%. One precursor was selected each cycle; each precursor was excluded after 3 spectra; the release time was 0.3 min. All collision-induced fragmentation experiments were performed in the ion-trap with helium as the collision gas, and the voltage was increased in cycles from 0.3 up to 2 V. The fragmentation time was 20 ms at an activation width of 10 u and the cut-off for the daughter ion range set at 30%. MS^3 data were obtained by manual fragmentation, targeting the most abundant ions in the precursor ion in the MS spectra.

Photostability experiments. The sunscreen mixtures with grape seed extract were prepared by adding about 20 mg of the sunscreen agents to 25 mL of the methanol extract (see Section on Sample preparation). This solution was then made up to 50 mL in a volumetric flask with methanol. To obtain working solutions, appropriate dilutions were carried out in order to obtain a sunscreen agent concentration of about 200 μmol dm^{-3} in the extract before photostability studies were performed.

Samples of grape seed extract with and without sunscreens added were exposed to simulated solar radiation in a Newport research lamp housing (M66901) fitted with a mercury-xenon lamp, powered by an arc lamp power supply (69911). The power output of the lamp was controlled by a digital exposure controller (68951) maintaining the output at 500 W m^{-2}. The output from the lamp was passed through a 10 mm-thick Pyrex filter to ensure that only wavelengths greater than 300 nm impinged on the samples. The exposure time was varied incrementally from 0 min in steps of 30 min to 240 min of continuous exposure. This gave an equivalent incremental standard erythemal dose (SED) (1 SED = 100 J cm^{-2}) of 2.16 to 17.3 SED. This work was carried out in Durban, South Africa, a region that receives daily total ambient erythemal ultraviolet radiation of about 60 SEDs during summer (26). Each exposed sample was contained in a stoppered 1.00 mm pathlength quartz cuvette. After each irradiation interval a UV-visible spectrum of the sample was recorded on a PerkinElmer Lambda 35 double beam UV-visible spectrophotometer. The percent photo-loss for the irradiated samples was calculated from the reduction in UV absorbance at the wavelength of maximum absorption of the specific absorbers or the observed maximum for the mixture (equation 1).

$$\%\ \text{photo-loss} = \frac{A_0 - A_t}{A_0} \times 100 \qquad \text{Equation 1}$$

where A_0 is the initial UV absorbance of the absorber and A_t is the absorbance after 240 min of

irradiation.

A 20 μL aliquot of these same solutions was then injected into the HPLC chromatograph to monitor the chemical transformations that took place. Samples of the sunscreens alone dissolved in methanol were similarly irradiated and monitored by UV-vis spectrophotometry and HPLC.

HPLC analysis of the irradiated samples. The chemical transformations in the irradiated samples were monitored on a Shimadzu Prominence LC chromatograph with a photodiode array detector. The chromatographic separation was achieved on an Agilent Zorbax Eclipse XDB C-18 reversed-phase column (150 × 4.6 mm, 5 μm particle size). For solutions of single UV filters the separations were conducted in the isocratic mode with a mobile phase of methanol-water in a ratio of 84:16 (% v/v). For the mixtures of the absorbers with grape seed extract the mobile phase was composed of water (solvent A) and acetonitrile (solvent B). The mixtures were resolved by a gradient elution as follows: 5–13 min, 16% B; 13-18 min, 45% B and held for 5 min; 23-28 min, 75% B, held for 5 min; 33-40 min, 99% B, then held for 5 min and subsequently dropped linearly to 16% B for 15 min. The experiment was performed at ambient temperature with a flow rate of 1 mL min^{-1} and an injection volume of 20 μL. The chromatograms were collected at detection wavelengths of 275, 280, 286, 310, 320 and 358 nm with a bandwidth of 4 nm simultaneously in each of the 60 min run time. The photodiode array detector was set to collect the UV-vis spectra of the chemical species separated over the range from 190 to 800 nm.

RESULTS AND DISCUSSION

Characterisation and photostability of the grape seed extract

The UV-vis spectrum of the grape seed extract showed absorbance in the UVC and UVB range and a very close similarity to the spectrum of catechin (27, 28) (Fig. 2). This observation was supported by HPLC analysis of the extract (see Supporting Information Fig. S1). The chromatogram detected at 280 nm exhibited one prominent broad peak with a similar UV spectrum to that of catechin (Fig. 2(a)). The broadness of this peak is a result of the co-elution of the two stereoisomers of catechin which could not be resolved under the current chromatographic conditions. However, both GC-FID and GC-MS analyses resolved the two isomers as epicatechin and catechin (see Fig. S2) at retention times of 31.970 and 32.581 min respectively, and showed very high amounts of these two stereomeric isomers of flavan-3-ols. Exposure of the grape seed extract dissolved in methanol to solar simulated radiation showed an increase in the absorbance with increasing irradiation time (Fig. 3(a)). This indicates an increase in photoprotection. The two isomers are known to undergo oligomeric polymerization catalysed by UV light to yield proanthocyanidins (Fig. 4). The observed phenomenon can be envisaged to be due to the polymerization of the oligomers in three fashions: either a *cis – cis, trans – trans* or *trans – cis* assembly of oligomers (Fig. 4). This results in different conjugation patterns that result in an increase in absorption extending to the UVA range. The linear increase in absorption capacity observed at 280 and 320 nm suggests that the same type of molecules come together in the same fashion to form the polymer achieving a linear reaction relation (Fig. 3(b)). From the linear increase in absorbance at 280 and 320 nm it is proposed that the molecules combine in a *cis-trans* configuration. This stereochemistry provides better conjugation and n to π^* and π to π^* electronic transitions are enhanced, thus increasing the

UV absorption in the UVA range. This is apparent from the prominent peaks detected at 320 and 358 nm on the HPLC chromatograms (Fig. 5).

The GC-MS analysis of the grape seed extract showed the presence of various fragments of polyphenols: phenolic acids, flavonoids, catechins, proanthocyanidins, and anthocyanins (see Fig. S3). The observed lower molecular weight polyphenols could be attributed to fragmentation of the catechins during derivatization. The HPLC-ESI-MS/MS fragmentation of catechin can be rationalized by first a retro-Diels Alder fragmentation for ring A and other subsequent fragments seem to involve only ring B (see Fig. S4). From the results of the GC-MS analysis we conclude that the grape seed extract contains various classes of phenolic compounds. Among these compounds are the phenolic acids which are simple molecules and form a diverse group that includes the widely distributed hydroxybenzoic and hydroxycinnamic acids (29). The isolated compounds: 3,4-dihydroxybenzoic acid, 3-hydroxy-4-methoxybenzoic acid and 2-(3,4-dihydroxyphenyl)-2-hydroxyacetic acid, can conveniently be associated with hydroxycinnamic acid derivatives. These compounds occur most frequently as simple esters with hydroxy carboxylic acids or glucose, and the hydroxybenzoic acid compounds are present mainly in the form of glucosides.

The 2-(3,4-dihydroxyphenyl)-3,4-dihydro-2H-chromene-3,5,7-triol identified from this extract is a flavonoid. This class of phenolic compound is widely distributed in nature and its polyphenolic structure makes these compounds very sensitive to oxidative enzymes (30). In this grape seed extract catechins were identified as the major constituents. Catechins are documented to mainly occur in tea leaves and grape seeds and the major monomeric flavan-3-ols present are: catechin, epicatechin, gallocatechin, epigallocatechin, epicatechingallate and epigallocatechin-3-gallate. The oligomeric polymerization of catechins produces

proanthocyanidins found in grape seeds, red wine and pine bark. The presence of these compounds in the extract under study leads us to expect that this extract exhibits reducing capacity and metal ion chelating ability like other polyphenols. The main cause of ROS generation in living tissues is the presence of metal ions and they play an important role in generation of oxidative stress, DNA damage and cell death. The biological properties of polyphenols depend on their molecular structure (31). The GC-MS results show the presence of benzene-1,2,3-triol commonly known as pyrogallol. This is a tri-functional benzene derivative positioning it as a powerful metal chelator, like catechol, for instance, which is a conjugate acid of a chelating agent used widely in coordination chemistry.

Apart from that, di-functional benzene derivatives like catechol, are known to readily condense to form heterocyclic compounds. It is well documented that catechol and gallol are effective metal ion chelators. Catechol reduces silver ions in solutions at ambient temperature and alkaline copper on heating (32-34). Consequently, the reactivities of proanthocyanidins and gallate esters with hydroxyl radicals, azide radicals, or superoxide anions correlate with catechol and pyrogallol groups in their molecular structures that provide evidence of the antioxidant properties of these agents (33). The scavenging activity of different grape catechin molecules is also related to the number of o-dihydroxy and o-hydroxyketo groups, C2-C3 double bonds, concentration and solubility, the accessibility of the active group to the oxidant and on the stability of the reaction product. Polyphenols also affect signal transduction pathways, modulate many endocrine systems, and alter hormones and other physiological processes, as a result of their binding to metal ions and enzyme cofactors. We envisage that coupled with the shown UVB absorbing potential of the extract in this work, the inclusion of

the grape seed extract in sunscreens is likely to boost the photoprotection and increase the antioxidant effect.

Photostability of EHMC in grape seed extract

The exposure of a methanolic solution of EHMC to solar simulated radiation showed the characteristic cinnamic acid moiety decay (Fig. 6 (a) and (c)). The HPLC analysis of this solution showed the formation of *cis*-EHMC (see Fig. S5) as the only photoproduct; this is in agreement with the findings of Broadbent et al. (35). The UV spectra in this work (Fig. 6 (a) and (c)) indicate an initial drop to a pseudo-photostationary state followed by a further drop in the UV absorption before attaining a relative stationary state in the fourth hour (Fig 6 (c)). A 35.0% photo-loss at 310 nm was observed after four hours of exposure (Table 1). The UV data is supported by the HPLC analysis that shows that the peak area of the *trans*-isomer for the 30 and 90 min exposure periods was nearly the same (56.2% and 53.0%, of the initial peak area respectively). When this chromatogram was monitored at 260 nm the *cis*-isomer shows greater absorption than the *trans*-isomer. This explains the loss in photoprotection attributed to this isomerisation of EHMC because this particular wavelength does not reach the earth's surface. However, when EHMC was combined with grape seed extract dissolved in methanol and exposed to solar simulated radiation for four hours, a new spectral decay characteristic was observed. The absorbance of this mixture dropped sharply after the first 30 min and subsequently stabilized for the remaining three and a half hours of exposure (Fig. 6 (b)). Thus, there is no further photo-loss and the extract improved the photostability by approximately 7.6% (Table 1). A plot of the HPLC peak areas of *cis*- and *trans*-EHMC monitored at 260 and 310 nm respectively indicated a decrease in the concentration of *cis*-EHMC after 30 min and

an increase in that of *trans*-EHMC (Fig 6 (d)). This could imply a speedy establishment of the photostationary state with higher preference for the *trans*-isomer (Fig 6 (c) and (d)). It could also be argued that there is no further transformation of the absorbing molecules but the HPLC chromatogram showed a number of peaks at 280 nm which could be associated with decay products arising from [2+2] cycloaddition (35, 36) of EHMC with other unsaturated secondary metabolites in the extract (Fig. 7). The [2+2] cycloaddition is usually accompanied by a reduction in double bond conjugation in the molecular structure of a compound and hence is likely to diminish the light absorption capacity of the molecule in question. The cyclobutane ring moieties formed are strained structures that are likely to breakdown in light-induced ring opening metathesis reactions yielding lower absorbing chemical species as observed in this work. Lack of the higher absorbing species from photo-induced reactions of the flavan-3-ols indicates no radical formation of catechins. This could imply that phenolics remain in their natural state; hence, better antioxidant activity is expected of this formulation. The formulation seems to have an efficient excited state self-deactivation mechanism by way of vibrational states depriving the molecules sufficient photon energy to combine and form other products. We do not rule out possible *cis-trans*-isomerization of EHMC but state that the decay life of the *cis*-EHMC is greatly reduced and thus likely to offer longer protection. From the UV spectra, the *trans*-isomer has a shoulder (~ 301 nm) which appears to vanish upon exposure to light. The overall effect is a stable sunscreen product, with antioxidant effect.

Photostability of BP3 in grape seed extract

The spectral stability of a BP3 solution in methanol was observed when irradiated with solar simulated radiation (Fig. 8 (a)). HPLC analysis of the irradiated solution did not show any other peaks thereby indicating that no photodegradation products are likely to be present (see Fig. S6). Similarly, methanolic solutions of BP3 with grape seed extract were exposed to simulated solar radiation for increasing exposure times without appreciable change in their UV spectra (Fig. 8 (b) and Table 1). This indicated good photostability of the agent in the plant extract. However, the HPLC chromatogram showed an additional two peaks observable at 280 and 358 nm (Fig. 9). These two peaks could be attributed to exclusive photo-reactivity of the benzophenone moiety albeit to a small extent. From a comparison of the UV spectra of BP3 in methanol (Fig. 8(a)) and in grape seed extract (Fig. 8 (b)) we note that one of the three peaks of the BP3 spectrum is missing in the latter, namely, that at 240 nm. This could be due to reactions involving BP3 induced by light that do not necessarily destroy the carbonyl chromophore, characterised by an absorption maximum at 286 nm. This could be the cause of the slight increase in absorption of 1.43% after irradiation (Table 1). This increase was also observed in the HPLC peak areas of BP3 monitored at 286 nm. It is known that upon irradiation of ketones, with radiation of wavelengths from 280 to 330 nm, an n to π^* transition takes place and because the triplet-singlet energy gap is small (20 - 70 kJ mol^{-1}) intersystem crossing occurs readily (37). We envisage that photochemical transformations lead to the formation of two UV-absorbing entities **A** and **B** exclusively from the triplet state of BP3 (Fig. 10 and Fig. S7). The high conjugation of species **B** makes it able to absorb at longer wavelength due to additional π to π^* transitions. The formation of these two species and other

absorbing chemical entities observed from the HPLC chromatographic results (Fig. 9) are unique to this grape seed extract and suggests synergistic UV absorption efficacy.

Schallreuter et al. (38) showed that BP3 is rapidly photo-oxidized, yielding benzophenone-3 semiquinone, a potent electrophile, capable of reacting with thiol groups on important antioxidant enzymes and substrates, such as thioredoxin reductase and reduced glutathione, respectively. This group argued that the rapid oxidation followed by the inactivation of important antioxidant systems indicates that this substance may be rather harmful to the homeostasis of the epidermis. But, from this work, given that its incorporation in the grape seed extract and subsequent prolonged UV exposure does not significantly alter the secondary metabolite composition, it can be argued that the grape seed extract is likely to modulate the photochemical response of BP3 and thereby improve its efficacy as a UV absorber.

Photostability of BMDBM in grape seed extract

BMDBM is a common sunscreen absorber incorporated in most cosmetics to protect human skin against deleterious UVA effects. In this work the irradiation of a solution of BMDBM in methanol showed a steady decay at 358 nm and an increase at 260 nm (Fig. 11 (a) and (c)). A 39.5% photo-loss was recorded at the end of the four-hour exposure period (Table 1). The *enol* tautomer of BMDBM has a maximum absorption at 358 nm and the *keto* tautomer shows a maximum around 260 nm. We therefore assign the decrease in absorption at 358 nm as *enol* decay and the observed growth at 260 nm as the increase of the *keto* tautomer. However, the HPLC chromatograms for the photostability studies did not show a marked loss of the *enol*-tautomer (see Fig S8). This apparent photostability could be due to a solvent effect because

BMDBM has been shown to be stable in polar protic solvents such as methanol (39). The *keto-enol* tautomerization is, therefore, accompanied by a loss in the photo-absorption efficacy of this sunscreening agent. BMDBM is also known to photodegrade upon irradiation in a nonpolar medium by way of radical formation (40) which may completely destroy its UV absorption potential. However, our photostability studies of a methanolic solution of BMDBM with grape seed extract over a four-hour illumination period showed a drop in the first 30 min and then relative photostability thereafter (Fig. 11 (b) and (c)). This mixture showed a much lower photo-loss (9.12%) after four hours of exposure than BMDBM alone (Table 1). A plot of absorbance against time indicated a relatively stable absorbing medium (Fig. 11 (c, line C). Similarly, there was no significant change in the HPLC peak areas of *enol*- and *keto*-BMDBM with increase in irradiation time in the presence of grape seed extract (Fig. 11 (d)). The spectra of the mixture extended to the visible region with the wavelength of maximum absorption shifting to 400 nm. From a comparison of the two sets of spectra, Fig. 11 (a) and 11 (b), we conclude that the incorporation of grape seed extract was the cause of the observed red shift. The shift towards much longer wavelength makes the mixture a better UV absorber and effectively covers the entire UVB and UVA spectrum. The UV spectra of the BMDBM and grape seed extract mixture (Fig. 11 (b)) showed an increase at 320 nm indicating the formation of other UV absorbing entities. This was supported by the HPLC chromatograms that showed very prominent peaks at 280 and 358 nm although the HPLC chromatographic data at 320 nm show these peaks to be smaller (Fig. 12). It can be concluded that these chemical species do not strongly absorb at 320 nm. Hence, the shift observed in the UV spectra is associated with photochemical reactions that yield strongly UV-absorbing species and since the spectral shape of BMDBM remains essentially the same, we conclude that the chelated *enol* form is

photostabilized. This observation in part agrees with the findings of Afonso et al. (22) who demonstrated that antioxidants may photostabilize BMDBM.

As indicated above BMDBM under UV irradiation is known to photodegrade into two radical species: a benzyl radical and a phenacyl radical (40). The presence of these radicals is likely to trigger free radical reactions especially given that flavan-3-ols at 300 nm are known to undergo homolysis of the heterocyclic 1,2-(O-C) and 3,4-(C-C) bonds (Fig. 13) (41). We speculate radical disproportionation reactions involving the benzyl and phenacyl radicals in the formation of the new photochemical products. We then invoke the Woodward-Fieser prediction rules for calculating the wavelength of maximum absorption in the UV for the proposed products to give λ_{max} values for compounds **K**, **R** and **X** (Fig. 12) as 325, 355 and 315 nm respectively and formed as shown in Figure 13. Our prediction agrees with the observed peaks detected by HPLC at 320 and 358 nm (Fig. 12 and Fig. S7). We therefore propose that the phenacyl radical couples with the catechin radical to give **X** and the benzyl radical couples with the catechin radical to give **K**. However, the photo-induced rearrangement of the catechin radical yields the long wavelength absorbing species **R** in a manner proposed by Fourie et al. (42). The other peaks appearing at 280 nm could result from various photo-induced radical disproportionation reactions in numerous fashions. The end result for this mixture of grape seed extract and BMDBM is a more effective and stable UV absorbing medium.

Photostability of a mixture of EHMC, BP3 and BMDBM in grape seed extract

It is common practice by most sunscreen product manufacturers to combine organic absorbers in a formulation with a view to producing a broad-spectrum product. The common combination is BMDBM for UVA absorption, EHMC for UVB and BP3 to provide a link between UVA and UVB. BP3 shows appreciable absorption in the UVA1 (320-340 nm) region (Fig. 8 (a)) and sufficient absorption in the UVB region and hence is considered as a suitable combination with any of the sunscreen agents. The irradiation of a methanolic solution of a mixture of EHMC, BP3 and BMDBM showed a steady spectral drop with increasing time of irradiation (Fig. 14 (a) and (c)). In this work, a 32.4% photo-loss was recorded for this mixture after a four-hour irradiation period (Table 1). The HPLC analysis showed a steady photoisomerisation of *trans*-EHMC to *cis*-EHMC (see Fig. S8). The BMDBM peak monitored at 358 nm, however, did not show any appreciable change in terms of peak area, indicating a degree of photostability (see Fig. S9). This could be attributed to solvent polarity because methanol is polar and protic, and such a medium has been shown to photostabilize BMDBM (39). Another notable observation on these spectra is the blue shift casting doubt on the UVA absorption potential of this mixture. It can be argued that in the absence of any other ingredient other than the three sunscreen absorbers, then this mixture is suitable for UVB photoprotection only. The photostability of a mixture of these three commonly used sunscreen absorbers in grape seed extract was investigated (Fig. 14 (b)). The three filters in the presence of the grape seed extract showed a broader coverage of the UV region. The photodegradation of this mixture was significantly reduced to 16.9% (Table 1). When the change in absorption with time was monitored at 305 nm, this mixture showed relative photostability after the initial drop (Fig 14 (c)). The observed drop in the presence of grape seed extract could be associated with

the initial decrease in *trans*-EHMC, which later stabilizes (Fig. 14 (d)). The three absorbers were mixed in the ratio 1:2:2, BMDBM:BP3:EHMC in accordance with the maxima allowed by COLIPA, namely, a percent composition of 5% BMDBM, 10% BP3 and 10% EHMC. A minimal drop in photo-absorption was observed in the first 30 min of exposure and subsequently the mixture was relatively photostable (Fig. 14 (c)). This shows that the inherent photoinstability of BMDBM and EHMC is diminished. The characteristic peaks observed, notably peak **R**, on the HPLC chromatogram (see Fig. 15) when the grape seed extract was exposed together with BMDBM, was also observed here (Fig. 15). This chemical species absorbs strongly in the UVA region. This indicates a few photo-induced radical reactions take place preferentially to BMDBM with the effect of increasing photostability in the UVA region. These radical disproportionation reactions have an effect of generating more UV-absorbing species thus avoiding the depletion of the antioxidant composition in the grape seed extract.

The observed absorption maxima of this mixture are in the UVB region and therefore this formulation is likely to offer sufficient UVB photoprotection (λ_{max} = 305 nm). Hence, a mixture of these sunscreens in grape seed extract may play a crucial role in minimizing UV-induced immunosuppression which is considered to be a risk factor for the development of skin cancer (43), and prevention of UV-induced immunosuppression represents a potential strategy for the management of skin cancer.

The aim of this work was to find a suitable combination of ingredients that affords a stable photoprotective product. This has direct consequences in terms of the possible ingestion of the product and hence safety concerns can be raised. Grape seed extract has been demonstrated to be non-genotoxic and to possess low toxicity as indicated by some *in-vitro* tests and *in-vivo* animal toxicity studies (13, 16, 44). Yakamoshi et al. (45) investigated the

acute and sub-chronic oral toxicity of grape seed extracts on Fischer 344 rats and for their mutagenic potential by the reverse mutation test on *Salmonella typhimurium*, the chromosomal aberration test on CHL cells, and the micronucleus test on ddY mice. This group found no evidence of acute oral toxicity at dosages up to an oral administration dose of 4 g kg^{-1}. There was no evidence of mutagenicity reported. From these studies we envisage that accidental ingestion of grape seed extract may pose neither an immediate or future grave danger. Additionally, in this work we have demonstrated the ability of grape seed extract to attenuate UV radiation and it's potential in reducing the adverse UV-induced effects on human skin. Proanthocyanidins, or condensed tannins, are said to have the capacity to stabilize collagen and elastin and thus enhance the elasticity, flexibility, and appearance of the skin (46). It is expected that UV-induced scars, stretch marks and skin wrinkling will be reduced. The observed stabilizing potential of the grape seed extract on the sunscreen chemical absorbers in combination and alone makes grape seed extract a good candidate as an ingredient in cosmetic formulations.

The secondary metabolites in grape seed extract undergo photochemical reactions yielding photoproducts that act synergistically and in combination with sunscreen absorbers to enhance photoprotection and improve broad-spectrum coverage. The photoinstability of the BMDBM and EHMC mixture is highly reduced when combined with grape seed extract. Although this study was performed in solution (methanol) and not in a formulation, the observed photostability of the filters in the presence of the extract is an indication of the likely improvement of photoprotection. We thus, propose that inclusion of grape seed extract in sunscreen formulations is likely to enhance the photoprotection potential of the formulation and minimise the need for additives in order to boost UV absorption efficacy. This will in turn

diminish the risk factor associated with undesirable formation of photoproducts whose toxicities are unknown in complex formulations. However, the performance of this extract in an actual formulation will depend on other factors such as the formulation type and preservatives added. These formulation characteristics need to be explored in the future.

ACKNOWLEDGEMENTS

This work has been supported by the CSIR National Laser Centre and MAO is grateful to the University of KwaZulu-Natal, College of Agriculture, Engineering and Science for the award of a doctoral bursary.

SUPPORTING INFORMATION

Additional Supporting Information is available in the online version of this article:

Figure S1. HPLC chromatogram of grape seed extract detected at 280 nm. The separation was achieved on a reversed-phase Zorbax Eclipse XDB C-18 column (150 mm × 4.6 mm, 5 µm), under a gradient elution of acetonitrile-water at a flow rate of 1 mL min^{-1} and an injection volume of 20 µL.

Figure S2. Total ion chromatogram of TMS-derivatized grape seed extract showing epicatechin and catechin. The separation was effected on a GL Sciences InertCap 5MS/Sil 30 m × 0.25 µm quartz capillary column under the conditions described in the Materials and Methods section.

Figure S3. Secondary metabolites identified in grape seed extract by GC-MS.

Figure S4. The proposed fragmentation of catechin and epicatechin in ESI-MS/MS (1, 2).

Figure S5. Isomerisation of EHMC under simulated solar irradiation monitored by HPLC at 260 and 310 nm on a reversed-phase Zorbax Eclipse-XDB C-18 column (150 mm × 4.6 mm) with methanol-water (84:16 % v/v) as the mobile phase. The injection volume was 20 µL and the flow rate was 1 mL min^{-1}.

Figure S6. The photostability of BP3 monitored by HPLC at 286 nm. The separation was achieved on a reversed-phase Zorbax Eclipse-XDB C-18 column (150 mm × 4.6 mm) with a mobile phase of methanol-water (84:16 % v/v). The injection volume was 20 µL and the flow rate was 1 mL min^{-1}.

Figure S7. The UV-visible spectra of the compounds formed when the grape seed extract was mixed with BP3 (compounds A and B) and when mixed with BMBDM (compounds K, R and X).

Figure S8. The photochemical changes of BMDBM monitored at 260 and 358 nm on a reversed-phase Zorbax Eclipse-XDB C-18 column (150 mm × 4.6 mm) with a methanol-water (84:16 % v/v) mobile phase. The injection volume was 20 µL and the flow rate was 1 mL min^{-1}.

Figure S9. The photochemical transformations of a mixture of EHMC, BP3 and BMDBM dissolved in methanol monitored by HPLC at 260, 286, 310 and 358 nm. The separation was effected on a reversed-phase Zorbax Eclipse-XDB C-18 column (150 mm × 4.6 mm). The mobile phase was a gradient elution of acetonitrile-water with a flow rate of 1.00 mL min^{-1} and an injection volume of 20 µL.

REFERENCES

1. Baliga, M. S. and K. S. Katiyar (2006) Chemoprevention of photocarcinogenesis by selected dietary botanicals. *Photochemistry and Photobiological Sciences* **5,** 243-253.

2. Sklar, L. R., F. Almutawa, H. W. Lim and I. Hamzavi (2013) Effects of ultraviolet radiation, visible light, and infrared radiation on erythema and pigmentation: a review. *Photochemical and Photobiological Sciences* **12,** 54-64.

3. Katiyar, K. S. (2008) Grape seed proanthocyanidines and skin cancer prevention: Inhibition of oxidative stress and protection of immune system. *Molecular Nutrition and Food Research* **52,** S71-S76.

4. Hruza, L. L. and A. P. Pentland (1993) Mechanisms of UV-induced inflammation. *Journal of Investigative Dermatology* **100,** 35S-41S.

5. Krause, M., A. Kilt, J. M. Blomberg, T. Soeborg, H. Frederiksen, M. Schlumpf, W. Lichtensteiger, N. E. Skakkebaek and K. T. Drzewiecki (2012) Sunscreens: are they beneficial for health? An overview of endocrine disrupting properties of UV-filters. *International Journal of Andrology* **35,** 424 - 436.

6. Bowden, G. T. (2004) Prevention of non-melanoma skin cancer by targeting ultraviolet-B-light signalling. *Nature Reviews Cancer* **4,** 23-35.

7. Koksal, E., E. Bursal, E. Dikici, F. Tozoglu and I. Gulcin (2011) Antioxidant activity of *Melissa officinalis* leaves. *Journal of Medicinal Plants Research* **5,** 217-222.

8. Mandal, P., T. K. Misra and M. Ghosal (2009) Free-radical scavenging activity and phytochemical analysis in the leaf and stem of *Drymaria diandra* Blume. *International Journal of Integrative Biology* **7,** 80-84.

9. DiGiovanni, J. (1992) Multistage carcinogenesis in mouse skin. *Pharmacology and Therapeutics* **54,** 63-128.

10. Baumler, W., J. Regensburger, A. Knak, A. Felgentrager and T. Maisch (2012) UVA and endogenous photosensitizers - the detection of singlet oxygen by its luminescence. *Photochemical and Photobiological Sciences* **11,** 107-117.

11. Ley, D. R. and A. Fourtanier (1997) Sunscreen protection against ultraviolet radiation-induced pyrimidine dimers in mouse epidermal DNA. *Photochemistry and photobiology* **65,** 1007-1011.

12. Maier, H., G. Schauberger, B. S. Martincigh, K. Brunnhofer and H. Hönigsmann (2005) Ultraviolet protective performance of photoprotective lipsticks: change of spectral transmittance because of ultraviolet exposure. *Photodermatology, Photoimmunology and Photomedicine* **21,** 84-92.

13. Khanna, S., M. Venojarvi, S. Roy, N. Sharma, P. Trikha, D. Bagchi, M. Bagchi and K. C. Sen (2002) Dermal wound healing properties of redox-active grape seed proanthocyanidins. *Free Radical Biology and Medicine* **33,** 1089-1096.

14. American Cancer Society (2008) Grapes. Accessed on 5 November 2014.

15. Kaur, M., R. Agarwal and C. Agarwal (2006) Grape seed extract induces anoikis and caspase-mediated apoptosis in human prostate carcinoma LNCaP cells: possible role of ataxia telangiectasia mutated-p53 activation. *Molecular cancer therapeutics* **5,** 1265-1274.

16. Bagchi, D., M. Bagchi, S. J. Stohs, D. K. Das, S. D. Ray, C. A. Kuszynski, S. S. Joshi and H. Pruess (2000) Free radicals and grape seed proanthocyanidin extract: importance in human health and disease prevention. *Toxicology* **148,** 187-197.

17. Svobodova, A., J. Psotova and D. Walterova (2003) Natural phenolics in the prevention of UV-induced skin damage. A review. *Biomedical Papers* **147,** 137-145.

18. Steinmetz, K. A. and J. D. Potter (1996) Vegetables, Fruit, and Cancer Prevention: A Review. *Journal of the American Dietetic Association* **96,** 1027-1039.

19. Scalbert, A. and G. Williamson (2000) Dietary intake and bioavailability of polyphenols. *Journal of Nutrition* **130,** 2073S-2085S.

20. Joshi, S. S., C. A. Kuszynski and D. Bagchi (2001) The cellular and molecular basis of health benefits of grape seed proanthocyanidin extract. *Current Pharmaceutical Biotechnology* **2,** 187-200.

21. Bagchi, D., A. Garg, R. L. Krohn, M. Bagchi, M. X. Tran and S. J. Stohs (1997) Oxygen free radical scavenging abilities of vitamins C and E, and a grape seed proanthocyanidin extract *in vitro*. *Research Communication on Molecular Pathology and Pharmacology* **95,** 179-189.

22. Afonso, S., K. Horita, J. P. Sousa e Silva, I. F. Almeida, M. H. Amaral, P. A. Lobão, P. C. Costa, S. M. Miranda, C. G. J. Esteves da Silva and J. M. Sousa Lobo (2014) Photodegradation of avobenzone: Stabilization effect of antioxidants. *Journal of Photochemistry and Photobiology B: Biology* **140,** 36-40.

23. Sudheer, K. M., S. B. Manjeshwar and K. S. Katiyar (2006) Grape seed proanthocyanidins induce apoptosis and inhibit metastasis of highly metastatic breast carcinoma cells. *Carcinogenesis* **27,** 1682-1691.

24. Cronin, H. and D. Z. Draelos (2010) Top 10 botanical ingredients in 2010 anti-aging creams. *Journal of cosmetic dermatology* **9,** 218-225.

25. Thornfeldt, C. (2005) Cosmeceuticals Containing Herbs: Fact, Fiction, and Future. *Dermatology and Surgery* **31,** 873-880.

26. Guy, C., R. Diab and B. Martincigh (2003) Ultraviolet Radiation Exposure of Children and Adolescents in Durban, South Africa. *Photochemistry and photobiology* **77,** 265–270.

27. Santos-Buelga, C., S. Bravo-Haro and J. C. Rivas-Gonzalo (1995) Interactions between catechin and malvidin-3-monoglucoside in model solutions. *Zeitschrift Fur Lebensmittel-Untersuchung und-Forschung* **201,** 269-274.

28. Plumb, G. W., S. De Pascual-Teresa, C. Santos-Buelga, V. Cheynier and G. Williamson (1998) Antioxidant properties of catechins and proanthocyanidins: Effect of polymerisation, galloylation and glycosylation. *Free Radical Research* **29,** 351-358.

29. Dai, J. and R. J. Mumper (2010) Plant Phenolics: Extraction, Analysis and Their Antioxidant and Anticancer Properties. *Molecules* **15,** 7313-7352.

30. Ghafar, M. F. A., K. N. Prasad, K. K. Weng and A. Ismail (2010) Flavonoid, hesperidine, total phenolic contents and antioxidant activities from Citrus species. *African Journal of Biotechnology* **9,** 326-330.

31. Afaq, F. and K. S. Katiyar (2011) Polyphenols: Skin Photoprotection and Inhibition of Photocarcinogenesis. *Mini Reviews in Medicinal Chemistry* **11,** 1200-1215.

32. Donovan, J. L., D. L. Luthria, P. Stremple and A. L. Waterhouse (1999) Analysis of (+)-catechin and (-)-epicatechin and their 3' - and 4' -O-methylated analogs a comparison of sensitive methods. *Journal of Chromatography B* **726,** 277-283.

33. Ferreira, D. and D. Slade (2002) Oligomeric proanthocyanidins: naturally occuring O-heterocycles. *Natural Product Reports* **19,** 517-541.

34. Soobrattee, M. A., V. S. Neergheen, A. Luximon-Ramma, O. I. Aruoma and T. Bahorun (2005) Phenolics as potential antioxidant therapeutic agents: mechanism and actions. *Mutation Research* **579,** 200-213.

35. Broadbent, K. J., B. S. Martincigh, W. M. Raynor, F. L. Salter, R. Moulder, P. Sjoberg and E. K. Markides (1996) Capillary supercritical fluid chromatography combined with atmospheric pressure chemical ionisation mass spectrometry for the investigation of photoproduct formation in the sunscreen absorber 2-ethylhexyl methoxycinnamate. *Journal of Chromatography A* **732,** 101-110.

36. Lyambila, W. (2003) A study of photoinduced transformations of sunscreen chemical absorbers. PhD Thesis, University of Natal, Durban, South Africa.

37. Wilkinson, F. (1997) Quenching of electronically excited states by molecular oxygen in fluid solution. *Pure and Applied Chemistry* **69,** 851-856.

38. Schallreuter, K. U., J. M Wood, D. W. Farwell, J. Moore and H. G. M. Edwards (1996) Oxybenzone oxidation following solar irradiation of skin: Photoprotection versus antioxidant inactivation. *Journal of Investigative Dermatology* **106,** 583 - 586.

39. Mturi, G. J. and B. S. Martincigh (2008) Photostability of the sunscreening agent 4-*tert*-butyl-4'-methoxydibenzoylmethane (avobenzone) in solvents of different polarity and proticity. . *Journal of Photochemistry and Photobiology A: Chemistry* **200,** 410-420.

40. Schwack, W. and T. Rudolph (1995) Photochemistry of dibenzoyl methane UVA filters Part 1. *Journal of Photochemistry and Photobiology B: Biology* **28,** 229-234.

41. Sisa, M., S. L. Bonnet, D. Ferreira and J. H. Van der Westhuizen (2010) Photochemistry of flavanoids. *Molecules* **15,** 5196-5245.

42. Fourie, T. G., D. Ferreira and D. G. Roux (1977) Flavanoid synthesis based on photolysis of flavan-3-ols, hydroxyflavanones, and 2-benzylbenzofuranones. *Journal of the Chemical Society, Perkin Transactions I***,** 125-133.

43. Wang, Z. Y., R. Agarwal, Z. C. Zhou, D. R. Bickers and H. Mukhtar (1991) Inhibition of mutagenicity in *Salmonella-typhimurium* and skin tumor initiating and tumor promoting activities in SENCAR mice by glycyrrhetinic acid - comparison of 18 alpha-stereoisomers and 18 beta-stereoisomers. *Carcinogenesis* **12,** 187-192.

44. Mantena, S. K., S. M. Baliga and K. S. Katiyar (2005) Grape seed proanthocyanidins induce apoptosis and inhibit metastasis of highly metastatic breast carcinoma cells. *Carcinogenesis* **27,** 1682-1691.

45. Yakamoshi, J., M. Saito, S. Kataoka and M. Kikuchi (2002) Safety evaluation of proanthocyanidin-rich extract from grape seeds. *Food and Chemical Toxicology* **40,** 599-607.

46. Bagchi, D., A. Garg, R. L. Krohn, M. Bagchi, D. Bagchi, J, J. Balmoori and S. J. Stohs (1998) Protective effects of grape seed proanthocyanidins and selected antioxidants against TPA-induced hepatic and brain lipid peroxidation and DNA fragmentation, and peritoneal macrophage activation in mice. *General Pharmacology* **30,** 771-776.

FIGURE CAPTIONS

Figure 1. Common proanthocyanidins and anthocyanidins found in grape seed (*Vitis vinifera*) extracts.

Figure 2. UV spectrum of (a) catechin (30) and (b) a 0.06 mg mL^{-1} solution of grape seed extract dissolved in methanol. The spectrum in (b) was acquired with a PerkinElmer Lambda 35 UV-Vis spectrophotometer in a 1 mm pathlength quartz cuvette with air as the reference.

Figure 3. (a) The photostability of 0.06 mg mL^{-1} grape seed extract dissolved in methanol, exposed to solar simulated radiation, in a 1 mm pathlength quartz cuvette. Each exposure cycle involved the use of a fresh sample of extract. The spectra were recorded on a PerkinElmer Lambda 35 UV-vis dual-beam spectrophotometer. (b) Increase in the photo-absorptive potential of grape seed extract dissolved in methanol at A: 280 nm and B: 320 nm.

Figure 4. Proposed polymerisation scheme of proanthocyanidins that enhance UV absorption.

Figure 5. Photochemical changes of a methanolic solution of grape seed extract monitored at 280, 320 and 358 nm showing the increasing catechin peak area with increase in irradiation time. The separations were achieved on a reversed-phase Zorbax Eclipse XDB C-18 column (150 mm × 4.6 mm, 5 µm), under a gradient elution of acetonitrile-water at a flow rate of 1 mL min^{-1} and an injection volume of 20 µL.

Figure 6. The photostability of (a) EHMC, and (b) EHMC with grape seed extract in methanol under solar simulated radiation. The spectra were acquired with a PerkinElmer Lambda 35 UV-vis dual-beam spectrophotometer in a 1 mm pathlength quartz cuvette with air as the reference. (c) The change in absorbance with time for (A) EHMC in methanol monitored at 310 nm, and (B) a mixture of EHMC and grape seed extract monitored at 310 nm. (d) The

concomitant change in HPLC peak area of *cis*-EHMC monitored at 260 nm and *trans*-EHMC monitored at 310 nm in the presence of grape seed extract.

Figure 7. Photochemical changes of a mixture of EHMC and grape seed extract monitored by HPLC at 280, 320 and 358 nm showing an increase in the catechin peak area with an increase in irradiation time and relatively stable EHMC. The separations were achieved on a reversed-phase Zorbax Eclipse XDB C-18 column (150 mm × 4.6 mm, 5 µm), under a gradient elution of acetonitrile-water at a flow rate of 1 mL min^{-1} and an injection volume of 20 µL.

Figure 8. Photostability of (a) BP3, and (b) BP3 with grape seed extract dissolved in methanol. The spectra were acquired with a PerkinElmer Lambda 35 UV-vis dual-beam spectrophotometer in a 1 mm pathlength quartz cuvette with air as the reference.

Figure 9. Photochemical changes of the BP3 and grape seed extract mixture monitored by HPLC at 280, 320 and 358 nm showing an increasing catechin peak area with increase of irradiation time and peaks of compounds A and B. The separations were achieved on a reversed-phase Zorbax Eclipse XDB C-18 column (150 mm × 4.6 mm, 5 µm), under a gradient elution of acetonitrile-water at a flow rate of 1 mL min^{-1} and an injection volume of 20 µL.

Figure 10. Proposed triplet state rearrangement of BP3 to yield UV-absorbing species A and B.

Figure 11. Photostability of (a) BMDBM, and (b) BMDBM with grape seed extract dissolved in methanol. The spectra were acquired with a PerkinElmer Lambda 35 UV-vis dual-beam spectrophotometer in a 1 mm pathlength quartz cuvette with air as the reference. (c) The change in absorbance with time for (A) *enol*-BMDBM monitored at 360 nm, (B) *keto*-

BMDBM monitored at 260 nm, and (C) a mixture of BMDBM and grape seed extract monitored at 360 nm. (d) The concomitant change in HPLC peak area of *keto*-BMDBM monitored at 260 nm and *enol*-BMDBM monitored at 358 nm in the presence of grape seed extract.

Figure 12. Photochemical changes of a BMDBM and grape seed extract mixture monitored by HPLC at 280, 320 and 358 nm showing an increasing catechin peak area with increase of the irradiation time and the emergence of UV-absorbing species K, R and X. The separations were achieved on a reversed-phase Zorbax Eclipse XDB C-18 column (150 mm × 4.6 mm, 5 μm), under a gradient elution of acetonitrile-water at a flow rate of 1 mL min^{-1} and an injection volume of 20 μL.

Figure 13. Proposed photo-induced radical disproportionation reactions of BMDBM photolysis products and triplet state flavan-3-ols.

Figure 14. Photostability of a mixture of (a) EHMC, BP3 and BMDBM, and (b) EHMC, BP3, BMDBM and grape seed extract dissolved in methanol. The spectra were acquired with a PerkinElmer Lambda 35 UV-vis spectrophotometer in a 1 mm pathlength quartz cuvette with air as the reference. (c) The change in absorbance with time for (A) a mixture of EHMC, BP3 and BMDBM in methanol monitored at 305 nm, and (B) a mixture of EHMC, BP3, BMDBM and grape seed extract monitored at 305 nm. (d) The concomitant change in HPLC peak area of *cis*-EHMC and *keto*-BMDBM monitored at 260 nm, *trans*-EHMC monitored at 310 nm and *enol*-BMDBM monitored at 358 nm in the presence of grape seed extract.

Figure 15. Photochemical changes of a mixture of EHMC, BP3, BMDBM and grape seed extract monitored by HPLC at 280, 320 and 358 nm showing an increasing catechin peak area with increase of irradiation time. The separations were achieved on a reversed-phase Zorbax

Eclipse XDB C-18 column (150 mm × 4.6 mm, 5 µm), under a gradient elution of acetonitrile-water at a flow rate of 1 mL min^{-1} and an injection volume of 20 µL.

Table 1. Percent photo-loss of UV absorbance monitored at the wavelength of maximum absorbance for sunscreen absorbers and their mixtures with grape seed extract after 240 min of exposure to solar simulated radiation.

UV absorber	Wavelength of maximum absorption/nm	% photo-loss after 240 min of irradiation
BP3	286	0.18
EHMC	310	35.0
BMDBM	360	39.5
EHMC + BP3 + BMDBM	305	32.4
GRAPE + BP3	286	-1.43
GRAPE + EHMC	310	27.4
GRAPE + BMDBM	360	9.12
GRAPE + EHMC + BP3 + BMDBM	305	16.9

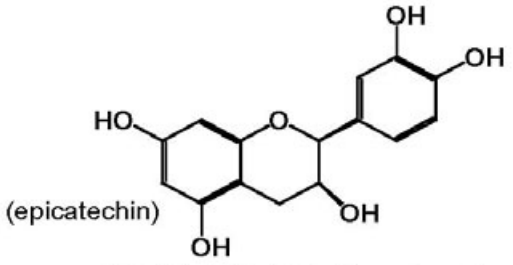

(2*S*,3*S*)-2-(3,4-dihydroxyphenyl)-3,4-dihydro-2*H*-chromene-3,5,7-triol

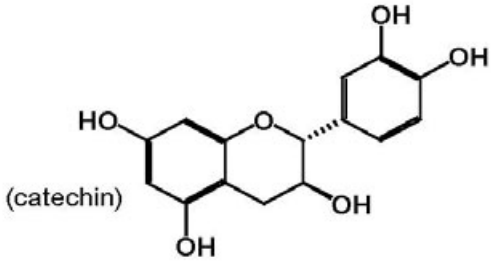

(2*R*,3*S*)-2-(3,4-dihydroxyphenyl)-3,4-dihydro-2*H*-chromene-3,5,7-triol

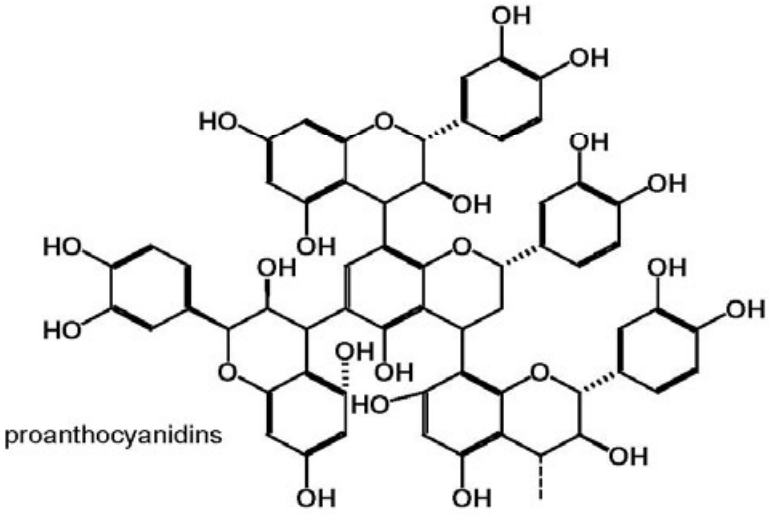

(2*R*,3*S*)-2-(3,4-dihydroxyphenyl)-4-((2*S*)-2-(3,4-dihydroxyphenyl)-4-((2*R*,3*S*,4*R*)-2-(3,4-dihydroxyphenyl)-3,5,7-trihydroxy-4-methyl-3,4-dihydro-2*H*-chromen-8-yl)-6-((2*S*,3*S*)-2-(3,4-dihydroxyphenyl)-3,5,7-trihydroxychroman-4-yl)-5-hydroxy-3,4-dihydro-2*H*-chromen-8-yl)-3,4-dihydro-2*H*-chromene-3,5,7-triol

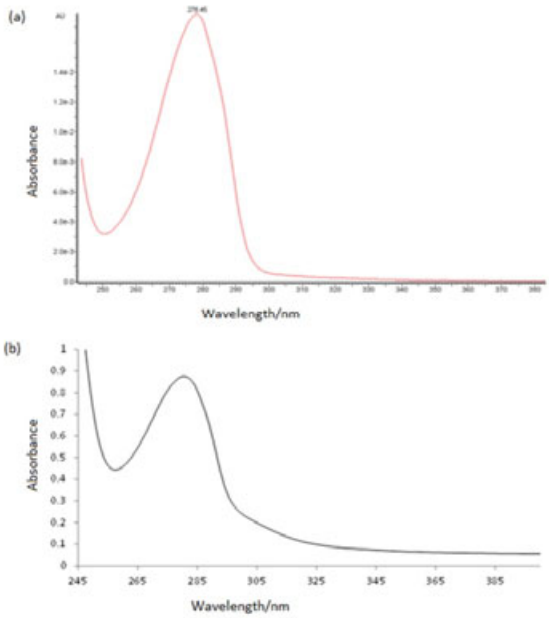

Figure 2

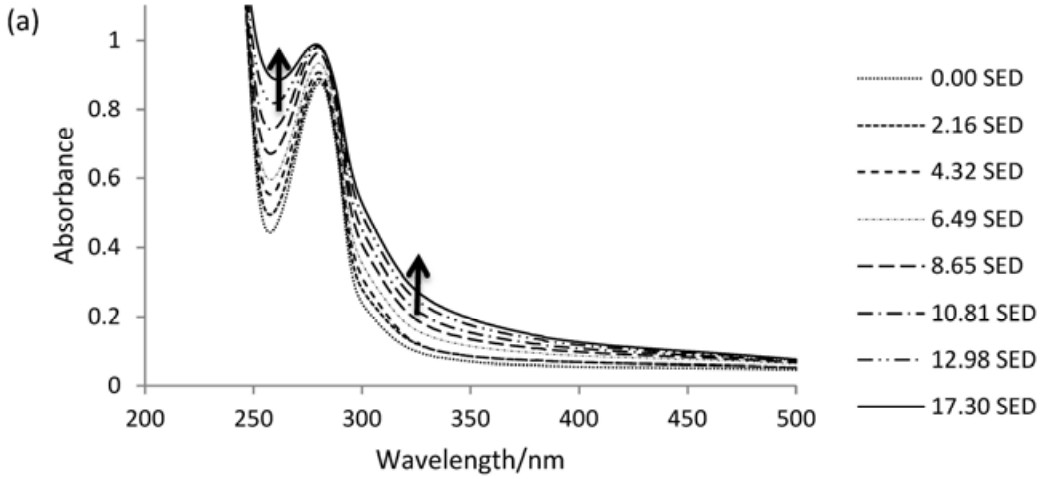

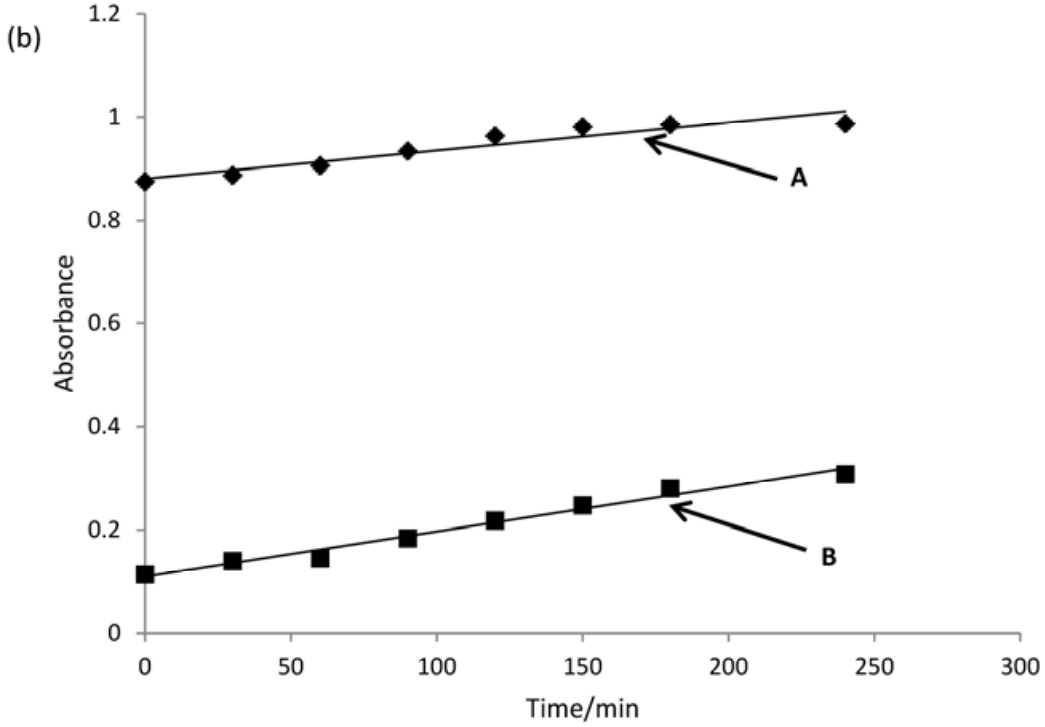

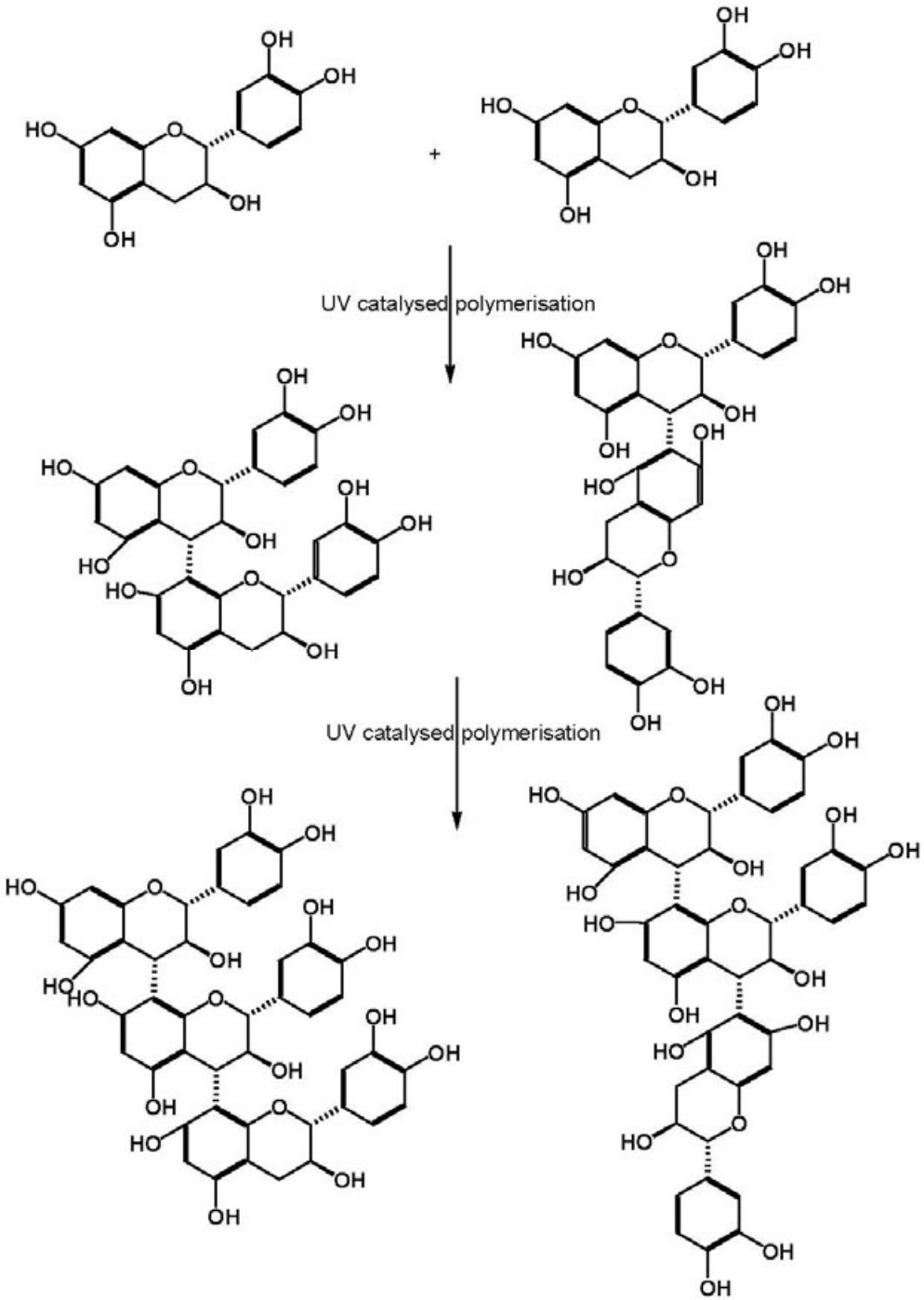

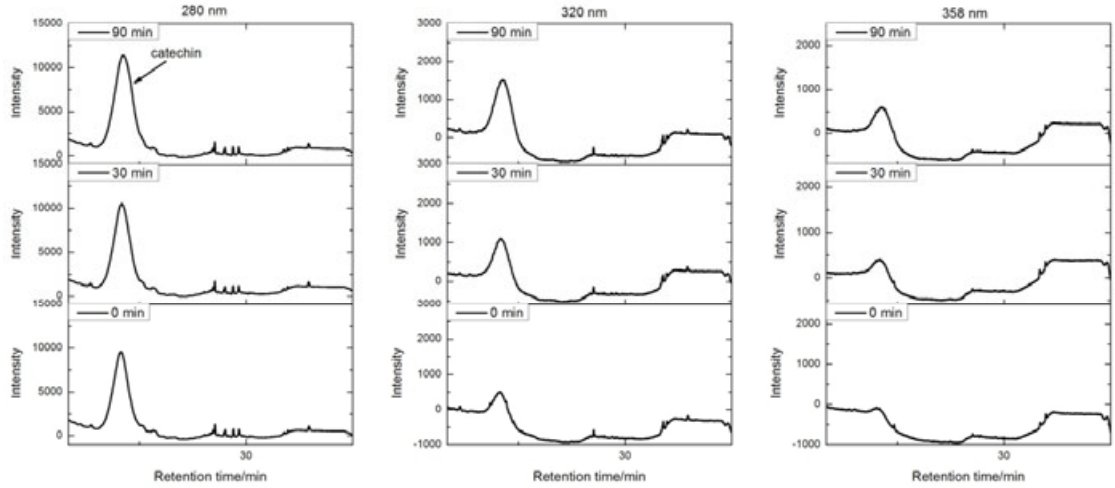

Figure 5

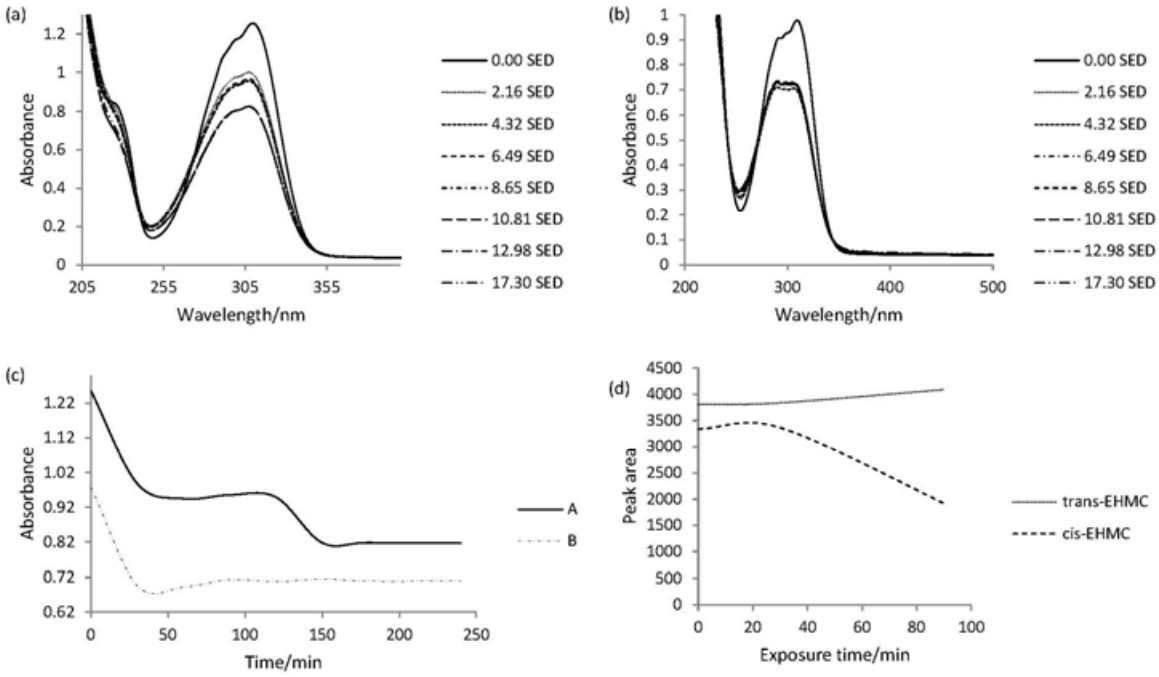

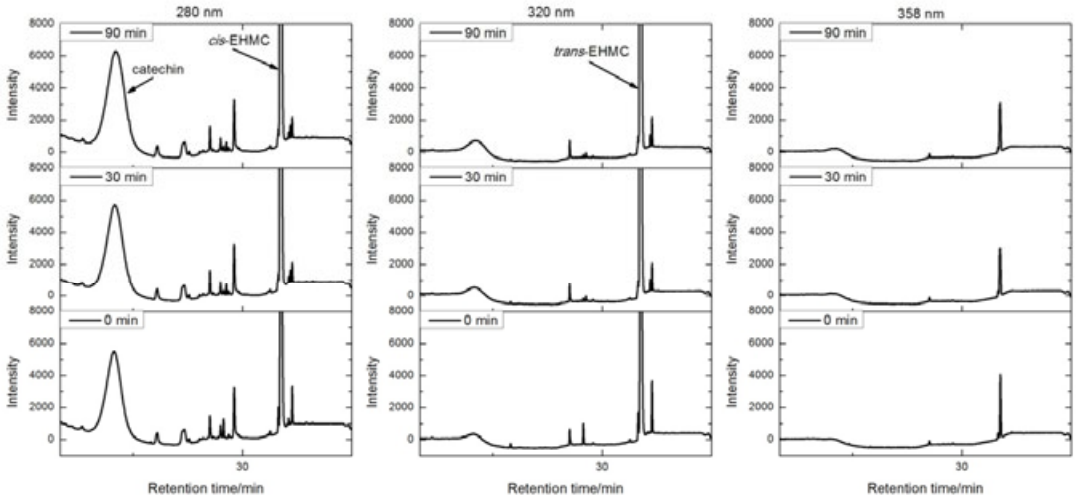

Figure 7

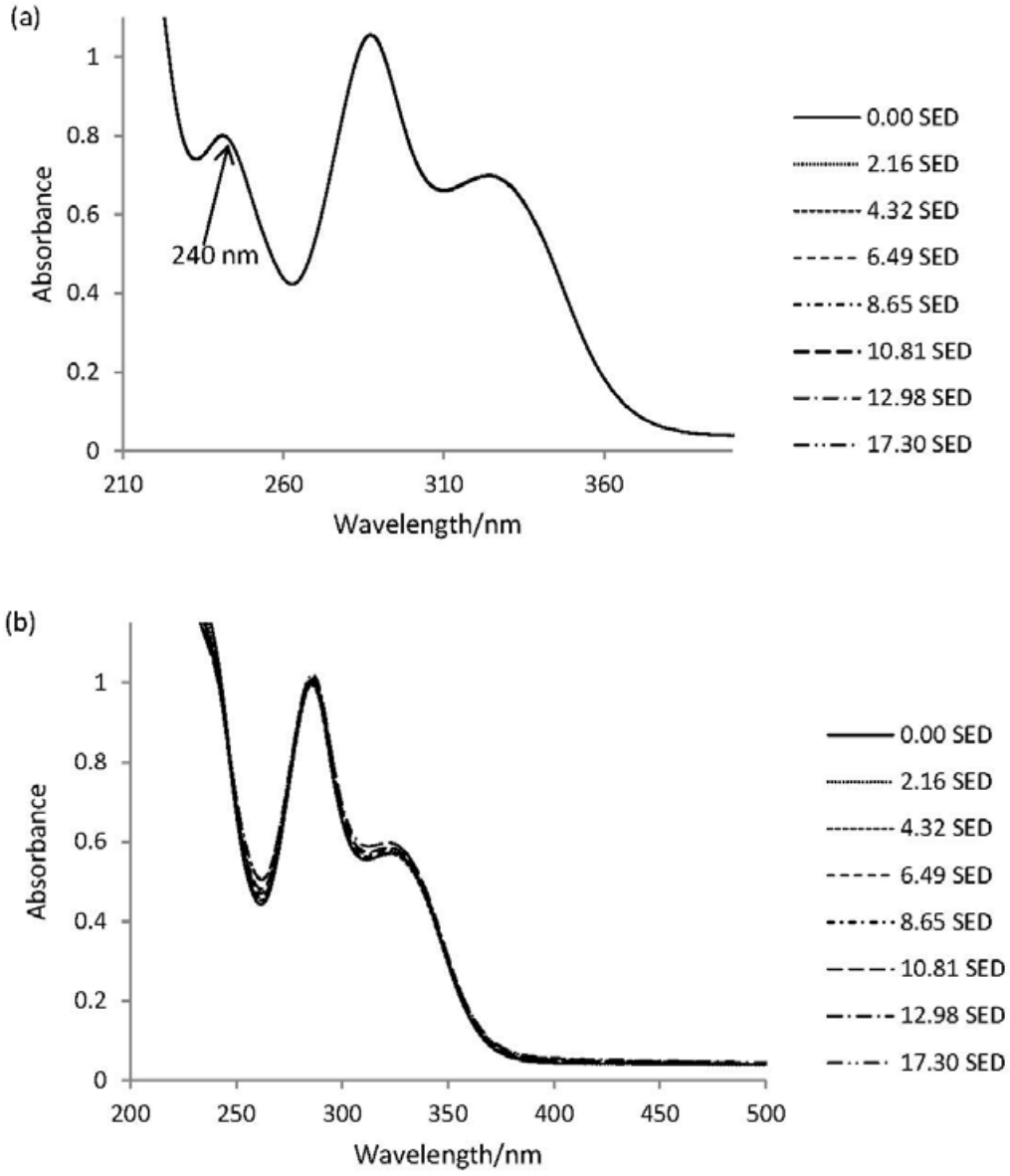

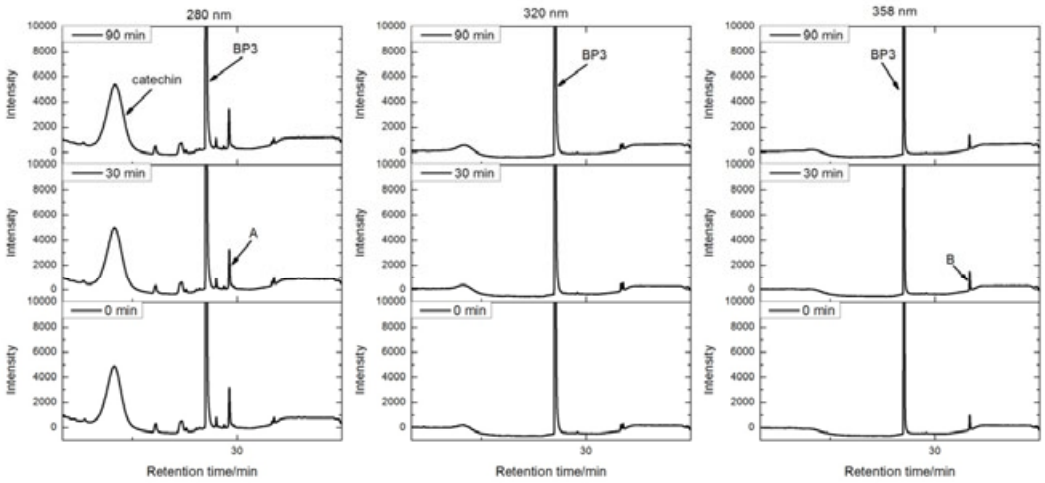

Figure 9

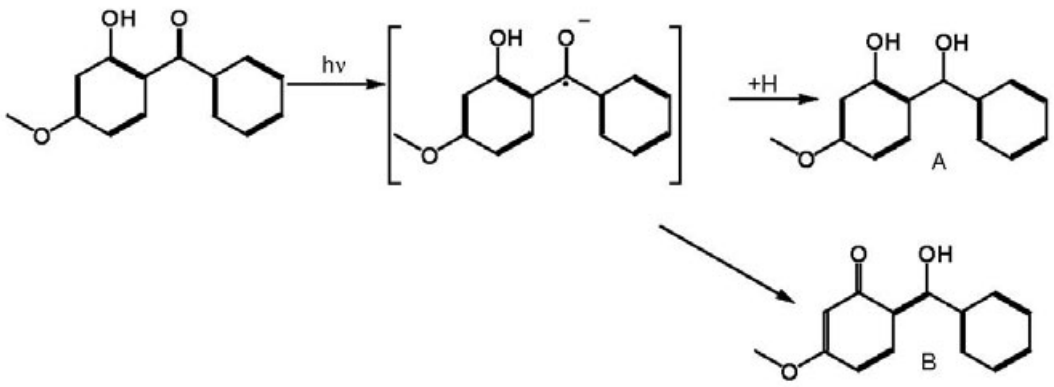

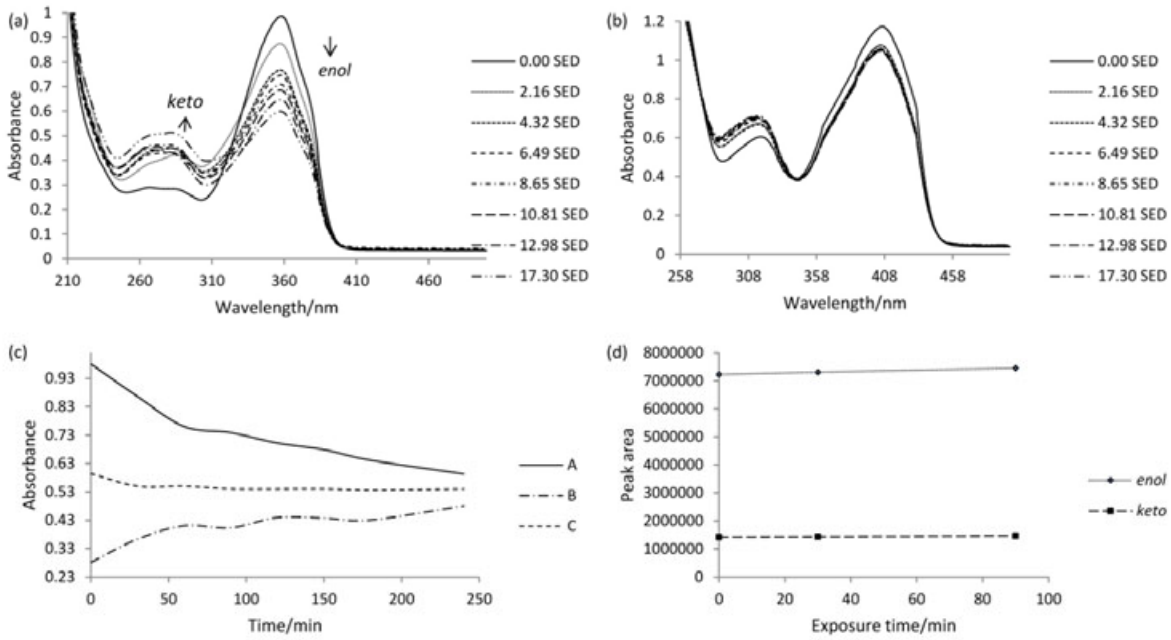

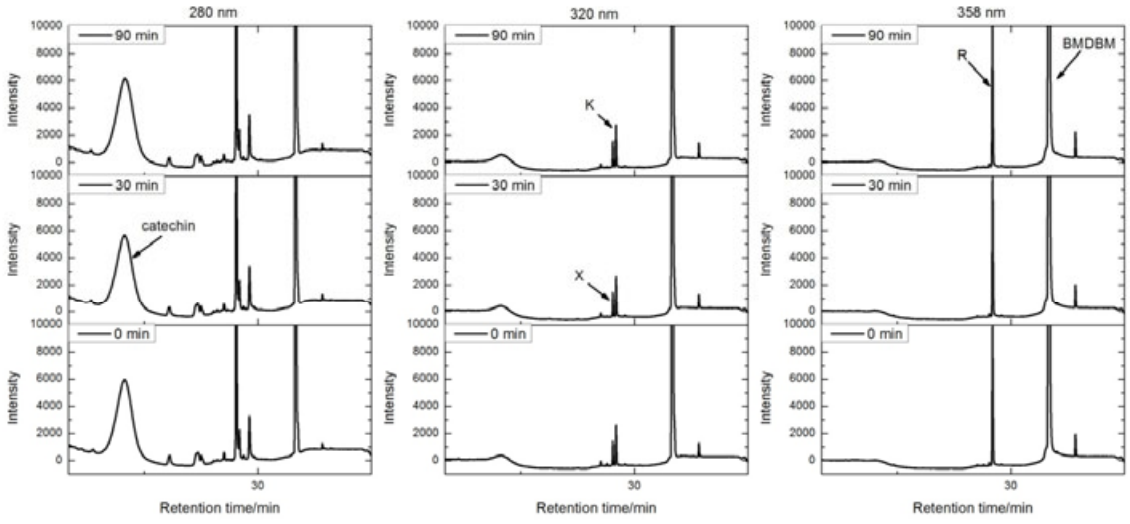

Figure 12

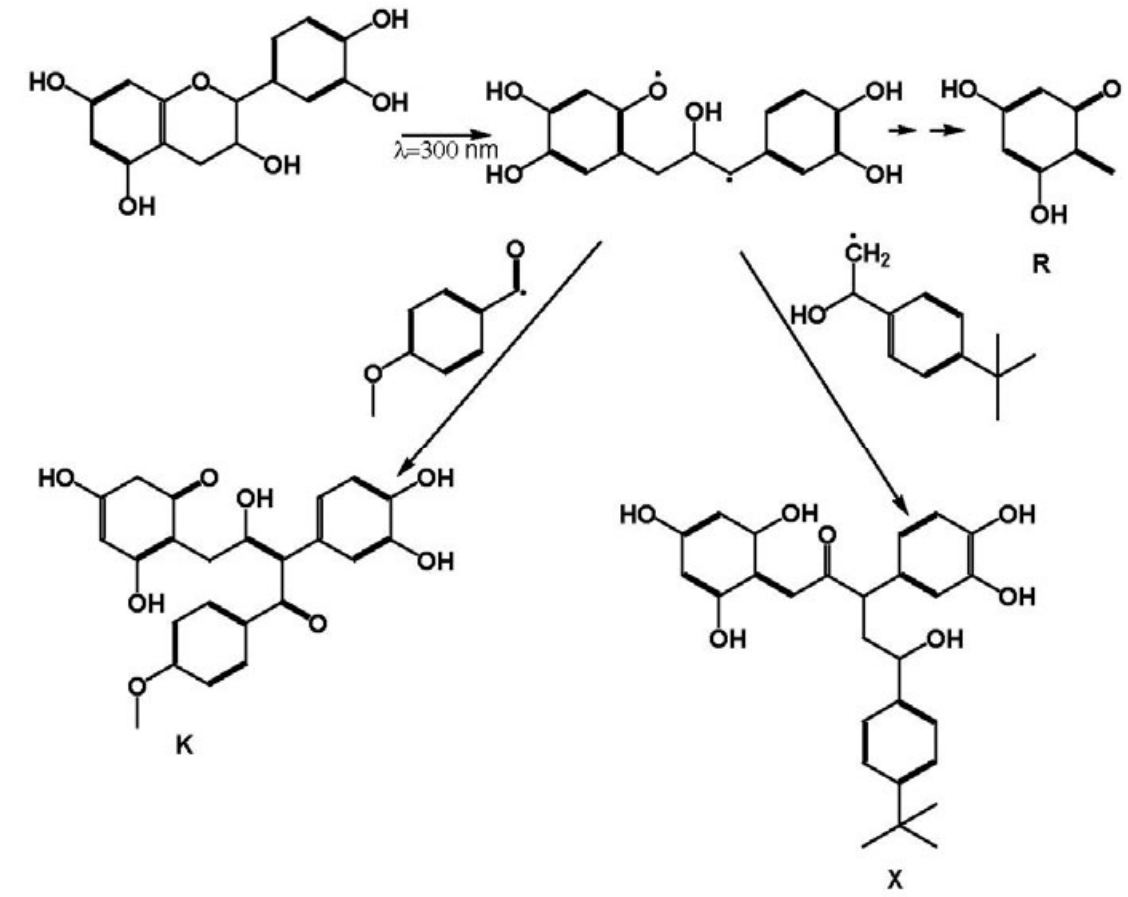

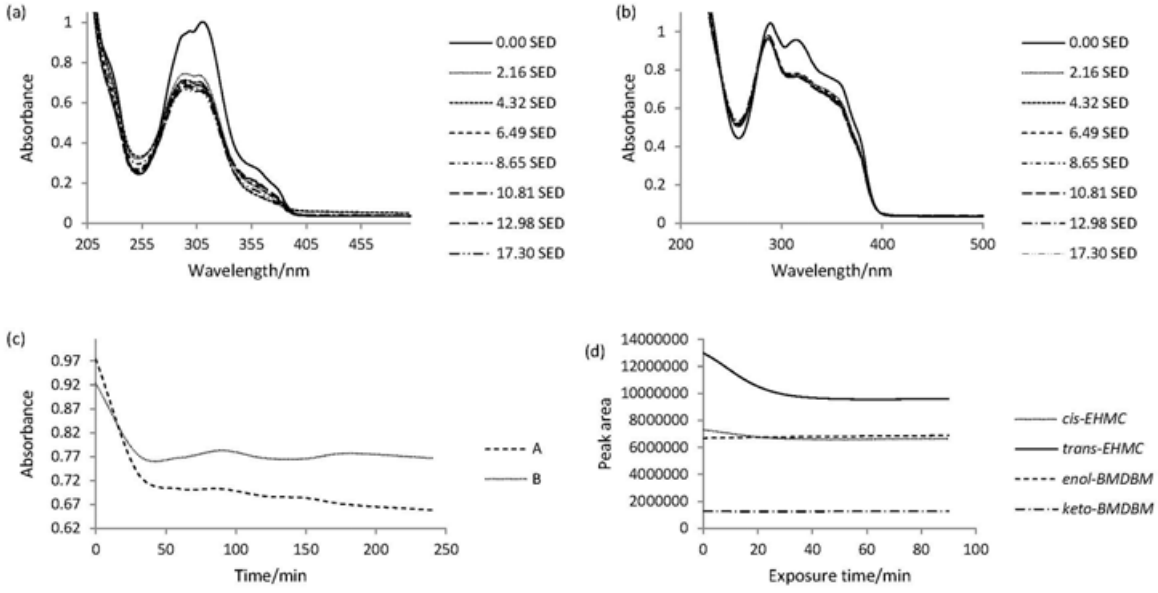

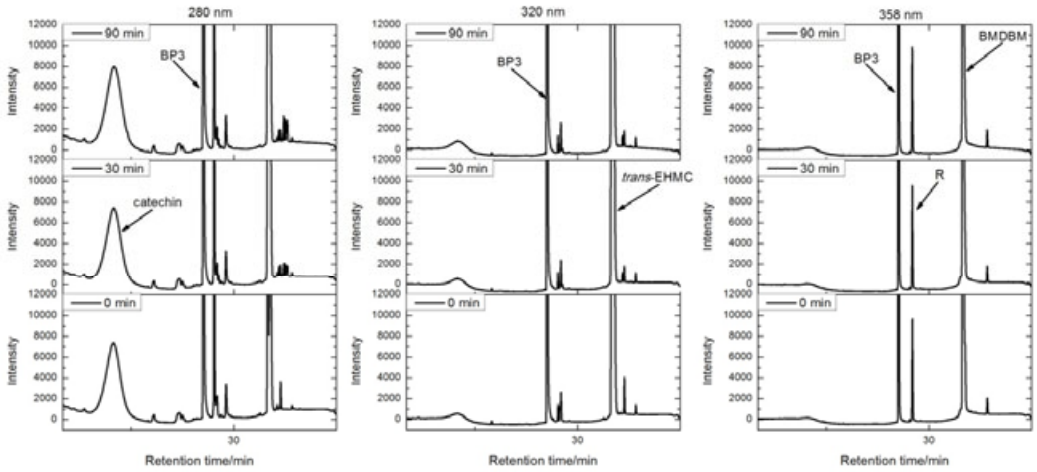

Figure 15